Pilot Reuse & Sum Rate Analysis of mmWave & UHF-based Massive MIMO Systems

Syed Ahsan Raza Naqvi, Syed Ali Hassan and Zaka ul Mulk

School of Electrical Engineering & Computer Science (SEECS)

National University of Sciences & Technology (NUST), Islamabad, Pakistan 44000

Email: {11beesraza, ali.hassan, 12mseezmulk}@seecs.edu.pk

Abstract—**In this paper, a pilot reuse scheme has been considered for the uplink (UL) transmissions of a massive multiple-input multiple-output (MIMO) system. Subsequently, a lower bound on the throughput of the system, that uses a maximal ratio combining (MRC) receiver, has been derived, which is applicable for any number of antennas. The throughput, along with other metrics, has been used to differentiate between the performance of ultra high frequency (UHF) and millimetre wave (mmWave) networks. The results indicate that the reuse factor plays a critical role in the least achievable throughput for UHF systems only, whereas the performance is almost independent for the mmWave networks.**

Index Terms—**Pilot contamination, UHF, mmWave, massive MIMO, MRC, average sum rate, throughput.**

I. Introduction

In conventional ultra high frequency (UHF) wireless cellular systems, multiple antennas are used at the BS providing a high throughput as well as improved quality of service to its users. Considering a multiple cell geometry, where each cell is equipped with tens of antennas making a massive multiple-input multiple-output (MIMO) system, it is obvious that the knowledge of channel state information (CSI) at the base station (BS) plays an important role to achieve high system performance. The most efficient way of obtaining CSI is through reciprocity that uses uplink (UL) training of pilots [1]. The major constraint while considering a multiple cell scenario using a UHF network, is the allocation of pilot signals to the users. This affects the system performance greatly as the CSI is further dependent upon the pilot allocation scheme. The frequent mobility of users shortens the channel coherence period and, as a result, the length of pilot sequence becomes limited. Therefore, considering the scarcity of bandwidth, it is not feasible to allocate distinct orthogonal pilot signals to users in each cell. The interference arising from the reuse of non-orthogonal pilot signals in different cells is commonly known as pilot contamination. It is known to limit the achievable throughput [2], and is caused when the CSI at BS is corrupted because of pilot signals from neighboring cells using the same frequency.

Marzetta [3] has shown in his work that as the number of antennas increases to infinity, the throughput eventually saturates, while [4] derives the asymptotic throughput bound, which shows that the throughput is limited by pilot contamination. Yang et al. [5] derived the throughput for a line geometry of cells where users are co-located in each cell.

As mentioned earlier, the primary bottleneck in assigning unique, orthogonal pilot signals to clients in each cell is the limited bandwidth offered by the UHF band. Greater bandwidth is also required to provide enhanced data-rates, a salient feature of the upcoming fifth generation (5G) technology. With a channel bandwidth of approximately 500 MHz and the possibility of using larger antenna arrays due to small wavelength [6], investigation into the use of millimetre wave (mmWave) technology in future cellular networks is already underway [7]. The subsequent discussion will aim to compare the performance of networks using UHF and mmWave technologies, considering not only the different bandwidths on offer, but also the distinct path loss models applied to transmissions in each system.

In this paper, a regular hexagonal geometry with random deployment of users is considered in order to study the impact of pilot contamination. Specifically, we study a conventional frequency reuse hex geometry and derive the throughput of the network. Finally, through simulations, relations between cell throughput, number of antennas, number of users per cell, pilot reuse factor and coherence period have been studied. It is shown that the reuse pattern has a strong impact on the system achievable throughput for UHF bands, whereas pilot reuse factor in mmWave has virtually no effect on pilot contamination.

II. System Model

Consider a tier-1 hexagonal geometry of a cellular system, where each cell has a radius, R. By tier-1, we refer to the area of interfering cells that causes co-channel interference (CCI) and is considered the main source of pilot contamination. The reuse factor of the hexagonal geometry is given by Q, where $Q = \{1, 3, 4, 7, ...\}$. For instance, in Fig. 1, six interfering cells for the center cell constitute tier-1 geometry with Q=1. Each cell contains an M-antenna BS that serves K randomly deployed single antenna mobiles. This paper will include scenarios with Q being equal to 1, 3 or 7. Next, we proceed to determining the 'path loss factor' for both UHF and mmWave networks. To this end, the path loss models for either system need to be defined. The path loss for mmWave link $L_{mm}(r)$, in dB, is modeled as,

$$L_{mm}(r) = \rho + 10\alpha \log(r) + \chi_{mm} \tag{1}$$
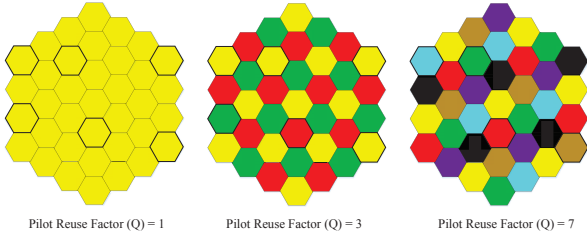
Fig. 1: Pilot reuse under consideration.

whereas the path loss for the UHF link, $L_{UHF}(r)$, in dB, is given by,

$$L_{UHF}(r) = 20 \log(\frac{4\pi}{\lambda_c}) + 10\alpha \log(r) + \chi_{UHF}, \quad (2)$$

In the above equations, χ_{mm} is the zero mean log normal random variables for the mmWave link, which models the effects of shadow fading. The fixed path loss in L_{mm} is given by $\rho = 32.4 + 20 \log(f_c)$ where f_c is the carrier frequency. The symbol χ_{UHF} represents the shadow fading in UHF links. The path loss exponents for both links are denoted by α.

Now, using these models, we extract the respective path loss factors for either system, which are given as,

$$\zeta_{i,j,k}^{mm} = 10^{-0.1(L_{mm}(r))} \quad (3)$$

$$\zeta_{i,j,k}^{UHF} = 10^{-0.1(L_{UHF}(r))}, \quad (4)$$

where $\zeta_{i,j,k}^{mm}$ is the path loss factor for the mmWave link and $\zeta_{i,j,k}^{UHF}$ is that for the UHF link. For the sake of generalization, all subsequent mathematical manipulations will use ζ to represent the path loss factor in both networks.

A Rayleigh block fading channel is assumed where all the channel coefficients remain constant for a block of T symbols; T being the channel coherence period. Considering the geometry, the channel matrix between the antenna i and mobiles in cell j is $\mathbf{C}_{i,j} \in \mathcal{C}^{M \times K}$ where all the entries of $\mathbf{C}_{i,j}$ are independent and identically distributed (i.i.d.) complex Gaussian with zero mean and unit variance. Fig. 1 also illustrates the mode of pilot reuse in the system under investigation, wherein each color represents a set of orthogonal pilots that are also mutually orthogonal from color to color. As a final remark, all the time/frequency resources allocated to payload data transmission are used in all the cells, as in [8].

III. MULTI-CELL UL COMMUNICATION

All users in this UL scenario communicate with their respective BS in two stages: UL training with pilot reuse and actual transmission of the data.

A. UL Training with Pilot Reuse

In each cell, orthogonal pilots are assigned to the users, which are reused by other cells by the factor Q. Assume a pre-designed pilot sequence matrix,

$$\boldsymbol{\Psi} = [\Psi_0, \cdots, \Psi_{Q-1}] \quad \in \mathbb{C}^{QK \times QK}, \quad (5)$$

where $\boldsymbol{\Psi}$ is divided among all cells. Assume that Ψ_0 is assigned to the Cell 0 which is considered to be the serving cell (center cell from Fig. 1) and the pilot sequence is further reused by Cell lQ where $1 \le |l| \le \lfloor \frac{L}{Q} \rfloor$ where L is the total number of cells in geometry. The pilot $\Psi_{q,k}$ is assigned to a single user k of a cell in order to remove intra-cell interference with the help of orthogonality of pilot signals.

We only analyze Cell 0 here for brevity. In a single time-frequency block, all the mobiles send their pilot signals to the BS. The signals received at BS 0 are,

$$\mathbf{P}_0 = \sqrt{\phi_\tau QK} \sum_{j=0}^{L-1} \mathbf{C}_{0,j} \, \Psi_{(j)}^* + \mathbf{W}_0, \quad \in \mathbb{C}^{M \times K}, \quad (6)$$

where $\mathbf{C}_{0,j} = [\zeta_{0,j,1}\mathbf{c}_{0,j,1}, \cdots, \zeta_{0,j,K}\mathbf{c}_{0,j,K}]$ is the channel matrix between the mobiles of cell j and BS 0, $\mathbf{c}_{0,j,k}$ is the channel vector between BS 0 and cell $j's$ k-th mobile user and $(j) = (j \mod Q)$. The variable $\mathbf{W}_0$ is i.i.d. $\mathcal{CN}(0,1)$ and ϕ_τ is the average transmission power per mobile. The factor $\sqrt{QK}$ guarantees that average power is ϕ_τ.

The received signal $\mathbf{P}_0$ is projected onto $\Psi_{0,k}$ in order to estimate $\mathbf{c}_{0,0,k}$ at the BS 0. After normalization, the resulting signals are,

$$\overline{\mathbf{p}}_{0,k} = \mathbf{c}_{0,0,k} + \sum_{l \neq 0} \sqrt{\frac{\zeta_{0,lQ,k}}{\zeta_{0,0,k}}} \mathbf{c}_{0,lQ,k} + \frac{\mathbf{w}_{0,k}}{\sqrt{\zeta_{0,0,k}\phi_\tau KQ}} \quad \in \mathbb{C}^{M \times 1}. \quad (7)$$

A minimum mean squared error (MMSE) estimator is applied to the received vector of pilots to get,

$$\hat{\mathbf{c}}_{0,0,k} = \mathbf{Y}_{cp} \mathbf{Y}_{pp}^{-1} \overline{\mathbf{P}}_{0,k}, \quad (8)$$

where $\mathbf{Y}_{pp}$ and $\mathbf{Y}_{cp}$ are the correlation and cross-correlation matrices, respectively. As all the channel vectors are independent therefore, the cross-correlation matrix becomes $\mathbf{Y}_{cp} = \mathbf{I}_M$. The correlation matrix $\mathbf{Y}_{pp}$ is given as

$$\mathbf{Y}_{pp} = \mathbf{I}_M + \underbrace{\sum_{l \neq 0} \frac{\zeta_{0,lQ,k}}{\zeta_{0,0,k}}}_{a_1} \mathbf{I}_M + \underbrace{\frac{1}{\zeta_{0,0,k} \, \phi_\tau KQ}}_{a_2}\mathbf{I}_M. \quad (9)$$

From the above equation, we can define $\sigma_\tau^2 = (1 + a_1 + a_2)^{-1}$ and now applying the MMSE decomposition

$$\mathbf{c}_{0,0,k} = \hat{\mathbf{c}}_{0,0,k} + \tilde{\mathbf{c}}_{0,0,k}, \quad (10)$$

where $\tilde{\mathbf{c}}_{0,0,k}$ is the independent uncorrelated estimation error. Both the entries are i.i.d. where $\hat{\mathbf{c}}_{0,0,k}$ is $\mathcal{CN}(0, \sigma_\tau^2)$ and $\tilde{\mathbf{c}}_{0,0,k}$ is $\mathcal{CN}(0, 1 - \sigma_\tau^2)$.

B. Actual Transmission of Data

In the next $T - KQ$ slots, all the mobiles transmit their data. This takes place in all cells after the UL training of pilots. The received signal at BS 0 is

$$\mathbf{r_0} = \sum_{j,k} \sqrt{\phi \zeta_{\mathbf{0},j,k}} \, \mathbf{c}_{\mathbf{0},j,k} \, r_{j,k} + \mathbf{n_0}, \quad (11)$$

where ϕ is the average power consumed by a mobile to transmit the data $r_{j,k}$ by a user k in cell j and $\mathbf{n}_o$ is the noise, which is $\mathcal{CN}(0,1)$. At BS 0, MRC is applied to receive the k-th mobile's signal. The unit norm vector is denoted as

$$\mathbf{u}_k = \frac{\hat{\mathbf{c}}_{0,0,k}}{\|\hat{\mathbf{c}}_{0,0,k}\|} \qquad \in \mathbb{C}^{M \times 1}. \tag{12}$$

After applying MRC and normalization, we get

$$\mathbf{u}_k^* \bar{\mathbf{r}}_0 = \mathbf{u}_k^* \hat{\mathbf{c}}_{0,0,k} \ r_{0,k} + \sqrt{\frac{1}{\phi_\tau \zeta_{0,0,k}}} w_k \tag{13}$$

$$+ \mathbf{u}_k^* \tilde{\mathbf{c}}_{0,0,k} \ r_{0,k} + \mathbf{u}_k^* \sum_{i \neq k} \sqrt{\frac{\zeta_{0,0,i}}{\zeta_{0,0,k}}} \mathbf{c}_{0,0,i} r_{0,i} \tag{14}$$

$$+ \mathbf{u}_k^* \sum_{j \neq 0} \sum_{i=1}^{K} \sqrt{\frac{\zeta_{0,j,i}}{\zeta_{0,0,k}}} \mathbf{c}_{0,j,i} r_{j,i}. \tag{15}$$

In (13), the two terms are the desired signal and the noise respectively. In (14), the terms signify the intra-cell interference and in (15), the term denotes inter-cell interference.

C. Achievable Cell Throughput

The average throughput of cell 0 using the above mentioned scheme is achieved by the derivation that follows. Tier-1 BSs of hexagonal geometry with M-antenna are deployed. Each BS serves K randomly located single antenna mobiles of its own cell with path loss factor $\zeta_{0,0,k}$.

The inter cell interference in (15) can be re-written as,

$$\mathbf{u}_k^* \sum_{j \neq 0} \sum_{i=1}^{K} \sqrt{\frac{\zeta_{0,j,i}}{\zeta_{0,0,k}}} \mathbf{c}_{0,j,i} r_{j,i} - \mathbf{u}_k^* \sum_{l \neq 0} \sqrt{\frac{\zeta_{0,lQ,k}}{\zeta_{0,0,k}}} \mathbf{c}_{0,lQ,k} r_{lQ,k}$$

$$+ \mathbf{u}_k^* \sum_{l \neq 0} \sqrt{\frac{\zeta_{0,lQ,k}}{\zeta_{0,0,k}}} \mathbf{c}_{0,lQ,k} r_{lQ,k}, \tag{16}$$

where the last term in (16) represents the pilot contamination. For a single user k, we can calculate the throughput as,

$$\mathcal{R}_k \geq \log_2 \left(1 + \frac{|\mathbf{u}_k^* \hat{\mathbf{c}}_{0,0,k}|^2}{\frac{1}{\phi \zeta_{0,0,k}} + I_1 + I_2 + I_3} \right), \tag{17}$$

where I_1, I_2, I_3 are intra-cell, inter-cell and interference due to pilot contamination.

We denote the rate conditioned on $\hat{\mathbf{c}}_{0,0,k}^*$, by $\bar{\mathcal{R}}$. To achieve the lower bound of $\bar{\mathcal{R}}$, convexity of $\log_2(1 + \frac{1}{x})$ is used. Following a series of mathematical manipulations, we get,

$$\bar{\mathcal{R}} \geq \log_2 \left(1 + \frac{|\mathbf{u}_k^* \hat{\mathbf{c}}_{0,0,k}|^2}{\frac{1}{\phi \zeta_{0,0,k}} + \mathbb{E}[I_1] + \mathbb{E}[I_2] + \mathbb{E}[I_3]} \right) \tag{18}$$

where $\mathbb{E}[I_1]$, $\mathbb{E}[I_2]$ and $\mathbb{E}[I_3]$ are given as,

$$\mathbb{E}[I_1] = (1 - \sigma_\tau^2) + \sum_{i \neq k} \frac{\zeta_{0,0,i}}{\zeta_{0,0,k}} \tag{19}$$

$$\mathbb{E}[I_2] = \sum_{j \neq 0} \sum_{i=1}^{K} \frac{\zeta_{0,j,i}}{\zeta_{0,0,k}} - \sum_{l \neq 0} \frac{\zeta_{0,lQ,k}}{\zeta_{0,0,k}} \tag{20}$$

$$\mathbb{E}[I_3] = \sum_{l \neq 0} \frac{\zeta_{0,lQ,k}^2}{\zeta_{0,0,k}^2} |\mathbf{u}_k^* \hat{\mathbf{c}}_{0,0,k}|^2 + \sum_{l \neq 0} \frac{\zeta_{0,lQ,k}}{\zeta_{0,0,k}} \left(1 - \frac{\zeta_{0,lQ,k}}{\zeta_{0,0,k}} \sigma_\tau^2\right). \tag{21}$$

It can be shown that $|\mathbf{u}_k^* \hat{\mathbf{c}}_{0,0,k}|^2$ has a gamma distribution with parameters (M, σ_τ^2). Following some manipulations, the right hand side of (18) is given by,

$$\bar{\mathcal{R}} \geq \log_2 \left(1 + \frac{(M-1)\sigma_\tau^2}{(\frac{1}{\phi \zeta_{0,0,k}} + \Omega_1 + \Omega_2 + \Omega_3)} \right), \tag{22}$$

where Ω_1 is the intra-cell interference, Ω_2 is the inter-cell interference and Ω_3 is the pilot contamination. The average achievable throughput for cell 0 is written as,

$$\mathcal{R} \geq K(1 - \frac{QK}{T}) \log_2 \left(1 + \frac{(M-1)\sigma_\tau^2}{\frac{1}{\phi \zeta_{0,0,k}} + \Omega_1 + \Omega_2 + \Omega_3} \right), \tag{23}$$

where ϕ is the average data power, T is the channel coherence period and σ_τ^2 is the normalized estimation power, where

$$\sigma_\tau^2 = \left(1 + \sum_{l \neq 0} \frac{\zeta_{0,lQ,k}}{\zeta_{0,0,k}} + \frac{1}{\sqrt{\phi_\tau KQ}} \right)^{-1}. \tag{24}$$

In (23), the constants Ω_1, Ω_2 and Ω_3 are defined as

$$\Omega_1 = (1 - \sigma_\tau^2) + \sum_{i \neq k} \frac{\zeta_{0,0,i}}{\zeta_{0,0,k}} \tag{25}$$

$$\Omega_2 = \sum_{j \neq 0} \sum_{i=1}^{K} \frac{\zeta_{0,j,i}}{\zeta_{0,0,k}} - \sum_{l \neq 0} \frac{\zeta_{0,lQ,k}^2}{\zeta_{0,0,k}^2} \sigma_\tau^2 \tag{26}$$

$$\Omega_3 = (M-1)\sigma_\tau^2 \sum_{l \neq 0} \frac{\zeta_{0,lQ,k}^2}{\zeta_{0,0,k}^2}. \tag{27}$$

IV. RESULTS

In this section, we evaluate the effect of interferences, pilot reuse factor and the number of users on the average cell throughput. For all simulations, we assume coherence period $T = 100$, radius $R = 800$m, and $\phi_t = \phi = 100$mW, unless noted otherwise. However, recent studies regarding the outdoor channel propagation characteristics for the mmWave network, referred to in [9], consider transmission links established for a distance of up to only 200–300m. The value of R is chosen only for a fair comparison between the two modes of transmission under investigation. All the mobiles in a UHF system operate at 3GHz frequency and 10MHz bandwidth. On the other hand, the mmWave network uses a carrier frequency of 94GHz and a bandwidth of 2GHz. The path loss exponents are assumed to be 3.8 for UHF, as in [5], and 3.3 for mmWave, as in [10], unless otherwise stated. In order to obtain ergodic
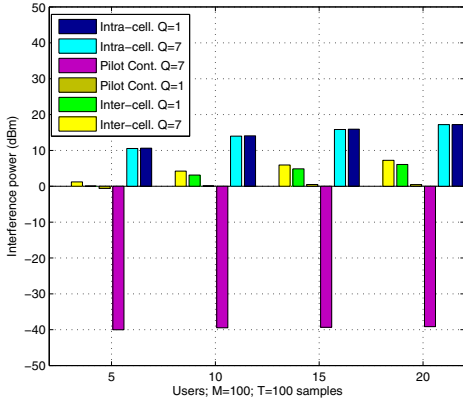
Fig. 2: Interference components in UHF systems using Q=1 and 7.
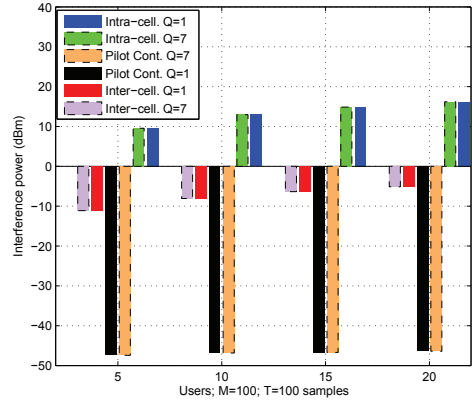
Fig. 3: Interference components in mmWave systems using Q=1 and 7.

cell throughput, the Monte-Carlo method has been applied for a single user having random location in every trial.

Since the mathematical manipulations of the previous section have provided us with expressions for not only the pilot contamination, but also the intra-cellular and inter-cellular interferences in the medium, we begin by contrasting the interference patterns in the networks under discussion.

The first graph, shown in Fig. 2, displays the said information for the UHF link for 5, 10, 15 and 20 users per cell, with the number of antennas, M, being fixed at 100. Note that the intra-cellular and the inter-cellular interferences increase steadily with an increase in the number of users for either value of Q. On average, both these interferences have the same impact on the throughput because the location of user is random; for distances closer to the BS, the intra-cell interference dominates and for distances far away, the inter-cell interference dominates. Hence, both generally have the same contribution to the cell throughput. It may also be seen that the pilot contamination has separate fixed values for the two reuse factors, independent of the total number of users. This is because, for tier-1, the number of interferers causing pilot contamination will always be six for any reuse factor. However, the figure clearly shows the potency of pilot reuse, as pilot contamination falls from approximately 0dBm for Q=1, to -40dBm for Q=7. Simply stated, the greater the value of the pilot reuse factor, the greater the distance of the interferer from the BS, resulting in a greater path loss experienced by the interfering signal and, hence, lesser pilot contamination.

Next, we consider the performance of the mmWave link in terms of interference for the same number of users and antennas, as shown in Fig. 3. The gradual increase in inter-cellular and intra-cellular interferences mirrors the trend seen previously in UHF systems. However, there are two other observations to be noted. Firstly, the inter-cellular interference in the mmWave network for both pilot reuse factors is much smaller than that seen in the previous graph. The reader may notice that there is a difference of nearly 10dBm in the inter-cellular interferences for the two systems at K=20, for either value of Q. Secondly, the pilot contamination is not only the
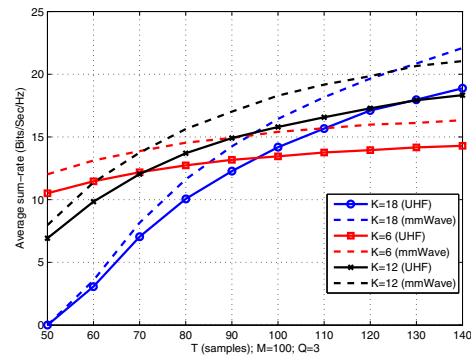
Fig. 4: Average throughput versus the coherence period for Q=3.

same for Q=1 and Q=7, but also remarkably smaller than that in Fig. 2. As an indicator, the pilot contamination for Q=1 is -48dBm, down from 0dBm for the UHF based communication. These results allude to the advantage afforded by the mmWave link's increased path loss, which drowns out the interference from the neighboring cells to the extent that a higher pilot reuse factor has no further impact on pilot contamination.

Now, we vary the coherence period in samples, T, while keeping Q fixed at 3. Fig. 4 plots the average sum rate against T for 6, 12 and 18 users in both UHF and mmWave networks. When we consider only 6 users in a cell, the throughput does not change much with the increase in T but when K goes to 18, the throughput starts increasing gradually as T increases. It can be seen that, for lower T, K=18 has the least performance. This is because, it is very difficult to generate orthogonal pilots for more users in lesser coherence period and hence the pilot contamination dominates the system. When T increases beyond a specific value, K=18 outperforms the rest of two cases. The mmWave system performs consistently better than that of UHF for the same value of K primarily due to decreased interference in the system.

Fig. 5 illustrates the relationship between the average throughput and M for both UHF and mmWave links, employing a pilot reuse factor of 3. As a preliminary observation, it may be stated that the sum rate is higher for greater values
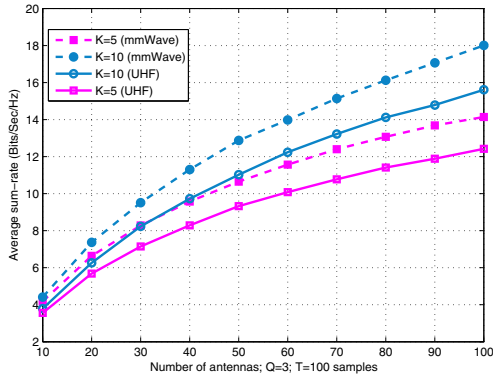
Fig. 5: Average throughput versus number of BS antennas at Q=3.
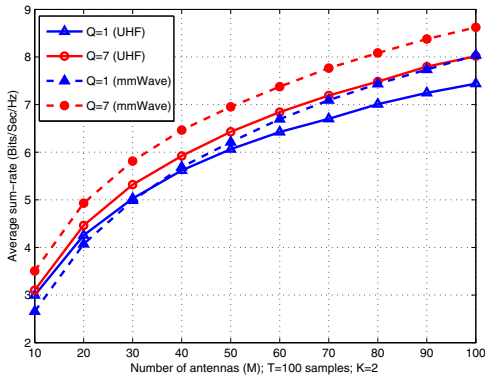
Fig. 6: Average throughput versus number of BS antennas at K=2.

of K, as M increases. Here again it may be noted that the mmWave network for the same value of K performs better than the UHF network under the assumed conditions, as explained previously. All plots start to approach saturation at higher values of M. Another point worth noting is that, at lower values of M, the performance of the mmWave system with 5 users per cell is nearly equivalent to that of the UHF system with 10 users per cell.

Extending the previous discussion, we now fix K at a low value and then observe the effect of Q, M and the mode of transmission on the system performance. The results are shown in Fig. 6. Once again, all plots start to approach saturation at higher values of M. Moreover, we see that the average sum rate for Q=1 for the mmWave link nearly equals that for the system operating at UHF with Q=7 at M=100.

Early on, it was mentioned that mmWave is a candidate for being the enabling technology of 5G networks due to its superior bandwidth as compared to UHF. We conclude this section by highlighting this very point. The data-sets in Fig. 7 were achieved by multiplying the results from (23) by the bandwidth of the respective transmission technique. As such, the average rate is measured simply in *Bits/Sec* in this case. It is obvious from the figure that the mmWave link outperforms the UHF link. Additionally, the plots for Q=1 and Q=3 for the mmWave network provide virtually similar results for all
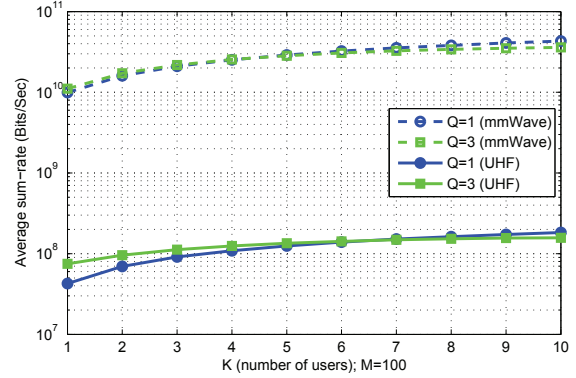
Fig. 7: Average throughput versus K.

values of K used. This further re-enforces the fact that at such high bandwidth, mmWave links need not incorporate pilot reuse into the network.

V. CONCLUSION

In this paper, we evaluated the lower bound for non-asymptotic throughput of an UL massive MIMO system with hexagonal geometry and random deployment of users, using MRC receivers. This expression was then used to gauge the performance of the mmWave and UHF links under similar conditions. It was observed that, for UHF, the effect of pilot contamination diminishes when the reuse factor is greater than 1. In contrast, mmWave shows very little variation in its already depleted pilot contamination levels for increased values of this factor.

REFERENCES

[1] T. L. Marzetta and B. M. Hochwald, "Fast transfer of channel state information in wireless systems," *IEEE Trans. Signal Process.,* vol. 54, pp. 1268-1278, 2006.
[2] J. Jose, A. Ashikhmin, T. L. Marzetta and S. Vishwanath, "Pilot contamination problem in multi-cell TDD systems," *IEEE International Symposium on Information Theory,* pp 2184-2188, July, 2009.
[3] T. L. Marzetta, "Noncooperative cellular wireless with unlimited number of BS antenna," *IEEE Trans. Wireless Commun.*, vol. 9, no. 11, pp. 3590-3600, Nov. 2010.
[4] B. Gopalkrishnan and N. Jindal, "An analysis of pilot contamination on multi-user MIMO cellular systems with many antennas," *IEEE SPAWC*, pp. 381-385, June 2011.
[5] Y. Li, Y. H. Nam, B. L. Ng and J. Zhang, "A non-asymptotic throughput for massive MIMO cellular UL with pilot reuse," *Wireless Communication Symposium - Globecom*, pp. 4500-4504, 2012.
[6] T. Bai, A. Alkhateeb, R. Heath, "Coverage and capacity of millimeter-wave cellular networks", *IEEE Commun. Mag.*, vol. 52, No.9, pp 70-77, September 2014.
[7] T. S. Rappaport, R. W. Heath Jr., R. C. Daniels, and J. N. Murdock, *Millimeter Wave Wireless Communication*, Prentice Hall, 2014.
[8] E. Bjornson, E. G. Larsson, M. Debbah, "Massive MIMO for maximal spectral efficiency: how many users and pilots should be allocated?," in *IEEE Trans. Wireless Commun.*, no. 99, pp. 1-16, Oct. 2015.
[9] W. Roh, J. Seol, J. Park, B. Lee, J. Lee, Y. Kim, J. Cho, K. Cheun, F. Aryanfar, "Millimeter-wave beamforming as an enabling technology for 5G cellular communications: theoretical feasibility and prototype results," in *IEEE Commun. Mag.*, vol. 52, no. 2, pp. 106-113, Feb. 2014.
[10] M. N. Kulkarni, S. Singh, J. G. Andrews, "Coverage and rate trends in dense urban mmWave cellular networks," in *IEEE Global Communications Conference (GLOBECOM)*, pp. 3809-3814, Dec. 2014.